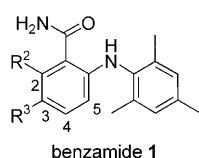


DOI: 10.1002/cmdc.201000253

## Design and Synthesis of Selective and Potent Orally Active S1P5 Agonists

Henri Mattes,<sup>\*,[a]</sup> Kumlesh Kumar Dev,<sup>[a, b]</sup> Rochdi Bouhelal,<sup>[a]</sup> Carmen Barske,<sup>[a]</sup> Fabrizio Gasparini,<sup>[a]</sup> Danilo Guerini,<sup>[a]</sup> Anis Khusro Mir,<sup>[a]</sup> David Orain,<sup>[a]</sup> Maribel Osinde,<sup>[a]</sup> Anne Picard,<sup>[a]</sup> Celine Dubois,<sup>[a]</sup> Engin Tasdelen,<sup>[a]</sup> and Samuel Haessig<sup>[a]</sup>

The immunomodulatory drug fingolimod (FTY720, 2-amino-2-[2-(4-octylphenyl)ethyl]propane-1,3-diol), derived from a fungal metabolite (ISP-1, myriocin), is phosphorylated *in vivo* by sphingosine kinases to produce (*R*)-FTY720-phosphate (FTY720-P).<sup>[1,2]</sup> FTY720-P activates sphingosine-1-phosphate (S1P) receptors S1P1, S1P3, S1P4, and S1P5 at low nanomolar concentrations and is inactive toward the S1P2 receptor.<sup>[1]</sup> The FTY720-P-mediated activation of the S1P1 receptor on lymphocytes induces receptor internalization, which attenuates T-cell response to S1P gradients, preventing their egress from secondary lymphoid tissues.<sup>[3]</sup> In addition to playing a role in the immune system, all S1P receptors except S1P4 are also found differentially expressed in the central nervous system<sup>[4]</sup> and on various tumor cell types.<sup>[5,6]</sup> Although the precise regulation of these receptors by locally released S1P remains unclear, S1P receptors are thought to play a role in such events as astrocyte migration,<sup>[7]</sup> oligodendrocyte differentiation, and cell survival<sup>[8,9]</sup> and neurogenesis.<sup>[10,11]</sup> To assess the relevance of individual S1P receptor subtypes for the activity of FTY720-P, selective agonists are required. Because S1P5 receptors are expressed on oligodendrocytes, and S1P5 receptors are thought to play a role in oligodendrocyte differentiation and survival, we focused on the development of S1P5 agonists. By using a high-throughput screening calcium mobilization assay with GPCR priming and FLIPR technology,<sup>[12]</sup> we discovered benzamide **1**, which has good *in vitro* potency toward the S1P5 receptor ( $EC_{50}$  = 270 nM), but has modest selectivity against S1P1 ( $EC_{50}$  = 3140 nM) and S1P4 ( $EC_{50}$  = 100 nM). Herein we report



our studies of various benzamide modifications carried out to improve the selectivity, bioactivity, pharmacokinetic properties, and ancillary profile of **1**, ultimately resulting in the discovery of potent and very selective S1P5 agonists.

To guide the optimization process, homology models of all S1P receptors were built from a crystal structure of bovine rhodopsin (PDB ID: 1F88).<sup>[13]</sup> Docking experiments of **1** into these models revealed a possible location of the binding site, some essential features of the interactions, and indicated potential regions for gaining selectivity and improving potency. In these complexes (Figure 1), **1** adopts a twisted conformation with the aniline ring, ~70° out of the benzamide plane and stabilized by a hydrogen bond between the aniline NH group and the amide carbonyl. In the S1P5 receptor complex, the amide group forms a hydrogen bond with OG1-Thr120. The benzamide phenyl ring lies in a large hydrophobic pocket surrounded by Phe196, Phe201, Phe268, Leu119, Trp264, Leu267, and Leu271. The aniline ring undergoes a T-shaped interaction with Phe116 and hydrophobic contacts with Leu271 and Leu292. The *ortho*-methyl substituents fill a small pocket formed by Tyr89, Val115, and Leu292 on one side, and sit at the face of Phe196 on the other side. Inspection of sequence alignments (Figure 2) revealed two positions, one in transmembrane (TM) helix TM3 (115, S1P5 sequence) and one in TM5 (192), where S1P5 has smaller residues lining the binding site, thus creating putative pockets. We hypothesized that filling these pockets with atoms from our ligands should lead to high selectivity for the S1P5 receptor. Position 2 on the benzamide core, which was closest to the hypothesized pocket around Val115, was therefore extensively modified.

Syntheses of derivative **1A–L** (Scheme 1) began with 3-fluorobromobenzene **2**, which was converted into acid **3** by reaction with lithium diisopropylamide (LDA) and carbon dioxide. Nucleophilic substitution of the fluorine atom with trimethylaniline at –78 °C yielded **4**. This intermediate was then used in various ways. Copper-catalyzed nucleophilic substitution of the bromine atom with various alcohols yielded ethers **5D–N**, which were amidated with ammonia using chlorodimethoxytriazine for activation to yield **1D–J**. Palladium-catalyzed substitution of the bromine atom in acid **4** with various alkylstannanes yielded **6A–C**, which were amidated as described above to yield **1A–C**. Alternatively, palladium-catalyzed substitution of the bromine atom with tributyl-(1-ethoxyvinyl)stannane yielded **9**, which was cyclized to **1L** by reaction with hydrazine. Acid **4** was also amidated with allylamine, using chlorodimethoxytriazine for activation, to yield allylamide **10**. Palladium-catalyzed cyclization of this intermediate led to **1K**.

All compounds were assayed for S1P5 activation in GTPγS assays,<sup>[13]</sup> which gave more reliable structure–activity results than the FLIPR assays, at concentrations up to 10 μM.  $EC_{50}$  values were determined for all compounds (Table 1). Disrupting the intramolecular hydrogen bond by introducing small alkyl substituents at position 2 (compounds **1A–C**), led to a

[a] Dr. H. Mattes, Prof. Dr. K. K. Dev, Dr. R. Bouhelal, Dr. C. Barske, Dr. F. Gasparini, Dr. D. Guerini, Dr. A. K. Mir, Dr. D. Orain, M. Osinde, A. Picard, C. Dubois, E. Tasdelen, S. Haessig  
Novartis Institute for Biomedical Research  
WKL-122 4002 Basel (Switzerland)  
Fax: (+41) 61 696 2455  
E-mail: henri.mattes@novartis.com

[b] Prof. Dr. K. K. Dev  
Molecular Neuropharmacology, Department of Physiology  
Trinity College Institute of Neuroscience (TCIN) Medical School  
Trinity College Dublin, Dublin 2 (Ireland)

Supporting information for this article is available on the WWW under <http://dx.doi.org/10.1002/cmdc.201000253>.

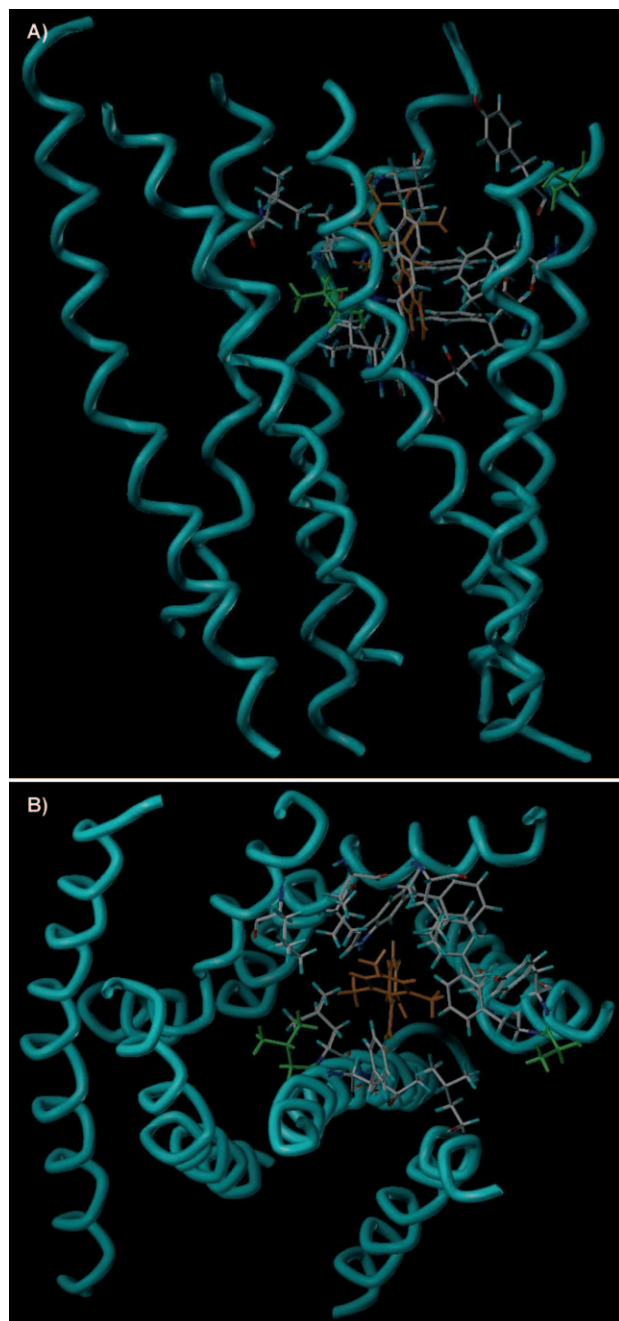
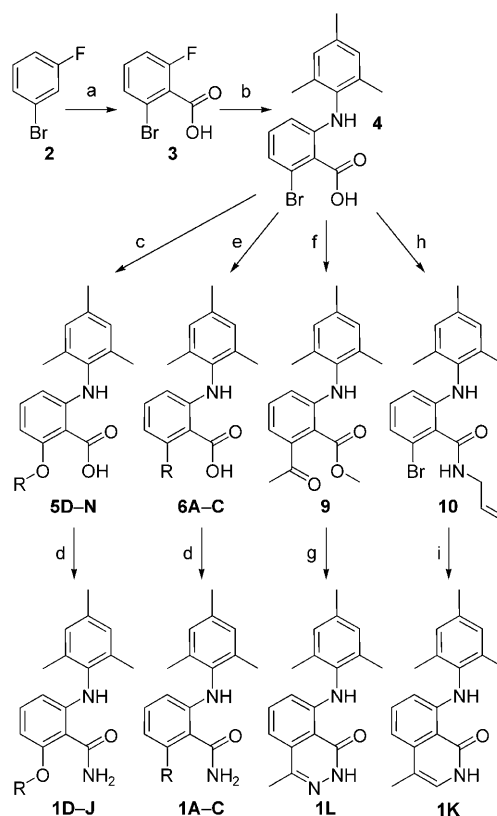


**Figure 1.** A) Longitudinal and B) transversal views of **1** (orange) docked into the S1P5 homology model. Residues Val115 and Ala192 are shown in green.

TM3	TM5	
PAQWFLREGS <b>MF</b> VA	HK <b>H</b> YILFCTTVFTL	S1P1
PTVWFLREGS <b>MF</b> VA	SK <b>K</b> YIAFCISIFTA	S1P3
PVQWFAREGS <b>AS</b> IT	AK <b>H</b> YVLCVVTIFSI	S1P2
PAQWFLREGL <b>L</b> FTA	SK <b>R</b> YILFCLVIFAG	S1P4
PALWFAREGG <b>V</b> FVA	AK <b>A</b> YVLCVLAFFVG	S1P5

**Figure 2.** Aligned sequences of S1P receptors. Position 115 (TM3, S1P5 sequence) and 192 (TM5) are highlighted in bold.



**Scheme 1.** Reagents and conditions: a) LDA (1.1 equiv), CO<sub>2</sub>, THF, -78 °C → RT; b) trimethylaniline (2.1 equiv), LDA (3 equiv), THF, -78 °C → RT; c) NaH (3 equiv), Cu (0.4 equiv), ROH/DMSO 5:1, 100 °C; d) chlorodimethoxytriazine (1.2 equiv), NMM (3 equiv), NH<sub>4</sub>OH (10 equiv), THF, RT; e) RSnBu<sub>3</sub> (1.5 equiv), Pd(PPh<sub>3</sub>)<sub>4</sub> (0.05 equiv), dioxane, 85 °C; f) 1. TMSCH<sub>2</sub>N<sub>2</sub>, MeOH, THF, RT; 2. tributyl-(1-ethoxyvinyl)stannane (1.5 equiv), Pd(PPh<sub>3</sub>)<sub>4</sub> (0.05 equiv), dioxane, 85 °C; g) NH<sub>2</sub>NH<sub>2</sub> (2 equiv), EtOH, 95 °C; h) chlorodimethoxytriazine (1.2 equiv), NMM (3 equiv), allylamine (1.5 equiv), THF, RT; i) Pd(OAc)<sub>2</sub> (0.05 equiv), tricyclohexylphosphine (0.1 equiv), *N,N*-dicyclohexylmethylamine (4 equiv), DMA, 60 °C, 24 h.

**Table 1.** S1P receptor profiles for selected derivatives of **1**.

Compd	R <sup>[a]</sup>	EC <sub>50</sub> [nM] <sup>[b]</sup>		
		hS1P5	hS1P1	hS1P4
<b>1A</b>	Me	685 (77)	> 10000 (62)	> 10000 (67)
<b>1B</b>	Pr	1155 (68)	> 10000 (4)	> 10000 (22)
<b>1C</b>	Pentyl	> 10000 (0)	> 10000 (0)	> 10000 (0)
<b>1D</b>	OMe	100 (79)	4067 (82)	1466 (73)
<b>1E</b>	OEt	72 (76)	> 10000 (26)	> 10000 (19)
<b>1F</b>	O <i>i</i> Pr	50 (75)	> 10000 (21)	> 10000 (16)
<b>1G</b>	O(CH <sub>2</sub> ) <sub>2</sub> OH	6 (99)	404 (78)	151 (126)
<b>1H</b>	O(CH <sub>2</sub> ) <sub>3</sub> OH	71 (93)	1001 (67)	4529 (119)
<b>1I</b>	O(CH <sub>2</sub> ) <sub>2</sub> OMe	113 (53)	5500 (63)	> 10000 (32)
<b>1J</b>		7 (95)	318 (85)	36 (152)

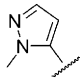
[a] See Scheme 1 for structures. [b] Values in parentheses indicate percent efficacy relative to FTY720-P; see Ref. [7] for details of GTPγS assays.

loss of agonist activity at all S1P receptors, in line with the conformational hypothesis delineated above. Conversely, introducing small alkoxy substituents at position 2 (compounds **1D–J**, **1M**, and **1N**), which would further stabilize an in-plane conformation of the amide, led to an improvement in agonist activity of the compounds at the S1P5 receptor. In line with our pocket hypothesis, slightly increasing the size of the alkoxy substituent also dramatically enhanced selectivity over other S1P receptors. Compounds **1E** and **1F** represent potent and exquisitely selective S1P5 agonists. Inverting the intramolecular hydrogen bond network by introducing an aniline at position 2 completely abolished agonist activity at all S1P receptors. Our models suggested that introducing hydrogen bond donors into the alkoxy substituents may yield additional binding affinity by interacting with OG-Ser122 or OD1-Asn128. This led to some very potent S1P5 agonists such as the hydroxyethoxy analogue **1G** and its stereochemically defined and conformationally constrained version, **1J**. However, such compounds displayed a slightly lower selectivity than the parent compound **1**. Given the necessity to keep the amide group in plane with the phenyl ring, a number of cyclic analogues of **1** were synthesized and tested (Table 2). In line with our models, the 3,4-

Compd <sup>[a]</sup>	EC <sub>50</sub> [nM] <sup>[b]</sup>		
	hS1P5	hS1P1	hS1P4
<b>1K</b>	41 (101)	357 (52)	607 (69)
<b>1L</b>	51 (87)	> 10 000 (41)	> 10 000 (79)

[a] See Scheme 1 for structures. [b] Values in parentheses indicate percent efficacy relative to FTY720-P; see Ref. [7] for details of GTP $\gamma$ S assays.

dihydro-2*H*-naphthalen-1-one derivatives and indan-1-one derivatives respectively exhibited low or no agonistic activity at the S1P5 receptor, highlighting the importance of the amide NH group. On the other hand, the 2*H*-isoquinolin-1-one derivative **1K** and the 2*H*-phthalazin-1-one derivative **1L** proved to be potent S1P5 agonists, with **1L** displaying very high selectivity over all other S1P receptors. Due to the significant increase in selectivity observed for benzamides with 2-alkoxy substituents, additional analogues were designed to further investigate substituents projecting into a hydrophobic pocket, which, according to our models, is located close to position 3 (Table 3). Incorporation of a 3-methyl or a 3-chloro group into **1D** dramatically increased potency, with **1M** and **1N** having respective EC<sub>50</sub> values of 2 and 13 nM at the S1P5 receptor. Both compounds still display good selectivity over the other S1P receptors. Further increasing the size of substituents at position 3 led to progressive loss of agonist activity at S1P receptors (data not shown). All compounds have lower selectivity than **1D**, a fact that can be explained by the apparent conservation of this pocket in all S1P receptors. Likewise, removing the substituent at position 2, while keeping one at position 3, led to some very potent S1P5 agonists such as **1O–Q**, which lack selectivity versus all other S1P receptors.

Compd	R <sup>2</sup>	R <sup>3</sup>	EC <sub>50</sub> [nM] <sup>[a]</sup>		
			hS1P5	hS1P1	hS1P4
<b>1M</b>	OMe	Me	2 (101)	476 (64)	373 (110)
<b>1N</b>	OMe	Cl	13 (77)	283 (84)	480 (117)
<b>1O</b>	H	Me	17 (86)	122 (95)	45 (106)
<b>1P</b>	H	<i>i</i> Pr	8 (90)	124 (91)	NT
<b>1Q</b>	H		1 (115)	10 (106)	NT

[a] Values in parentheses indicate percent efficacy relative to FTY720-P; see Ref. [7] for details of GTP $\gamma$ S assays; NT: not tested.

Based on their overall S1P receptor profiles, **1F** and **1L** were chosen for further profiling. Both compounds have good selectivity profiles with no apparent binding to a panel of more than 60 receptors and enzymes (data not shown). The compounds showed a low risk of hERG interaction, with IC<sub>50</sub> values > 30  $\mu$ M in the hERG cell-based assay. They also showed no substantial inhibition of all tested cytochrome P450 enzymes up to 10  $\mu$ M, making in vivo drug–drug interactions unlikely (data not shown).

Compound **1F** has rather low water solubility, ranging from 0.007 g L<sup>-1</sup> at pH 1 to 0.009 g L<sup>-1</sup> at pH 6.8, whereas moderate solubility, ranging from 0.058 g L<sup>-1</sup> at pH 1 to 0.037 g L<sup>-1</sup> at pH 6.8, was observed for **1L**. Furthermore, both compounds display good permeability as determined in the PAMPA and Caco2 assays, ranking them as class II compounds. Data regarding oral absolute bioavailability and disposition pharmacokinetics (PK) for **1F** and **1L**, as well as their in vivo brain penetration, were collected (Table 4). When tested in rats (10 mg kg<sup>-1</sup> p.o.), **1F** displayed low oral bioavailability, a relatively short half-life, moderate-to-high clearance, and good brain penetration. On the other hand, **1L** exhibited good PK properties, with a reasonable AUC (24 354 pmol mL<sup>-1</sup> h<sup>-1</sup>) and a good brain/plasma ratio of 3.8. In a study with a dose of 3 mg kg<sup>-1</sup> i.v., a rat plasma half-life of 7.4 h was observed, with a moderate volume of distribution ( $V_{dss}$  = 2.4 L kg<sup>-1</sup>) and a low

Compounds:	<b>1F</b>	<b>1L</b>
AUC [pmol mL <sup>-1</sup> h <sup>-1</sup> ] <sup>[a]</sup>	234	24 354
C <sub>max</sub> [pmol mL <sup>-1</sup> ] <sup>[a]</sup>	340	4343
Brain/plasma ratio (4 h i.v.) <sup>[b]</sup>	3.1	3.8
$t_{1/2}$ [h] <sup>[b]</sup>	2.8	7.4
CL [mL min <sup>-1</sup> kg <sup>-1</sup> ] <sup>[b]</sup>	68.1	12.3
$V_{dss}$ [L kg <sup>-1</sup> ] <sup>[b]</sup>	3.7	2.4
F [%]:	3	48

[a] 10 mg kg<sup>-1</sup> p.o. in NMP/Solutol/PEG-300 (5:10:85 v/v/v). [b] 3 mg kg<sup>-1</sup> i.v. in NMP/PEG (5:95 v/v).

clearance of  $CL = 12.3 \text{ mL min}^{-1} \text{ kg}^{-1}$ . These properties make **1L** a good candidate for further biological profiling.

From the five S1P receptors, S1P5 is best studied in oligodendrocytes, where it is thought to be involved in regulating oligodendrocyte differentiation and survival. The mRNA for S1P5 is predominantly expressed in the white matter tracts of the brain, including the cerebellum, corpus callosum, and the spinal cord.<sup>[14–19]</sup> S1P5 receptors are preferentially expressed in oligodendrocytes at all stages of development: progenitors and mature lineages.<sup>[9,17,20]</sup> The distinct distribution pattern of S1P5 suggests it may play an important role in regulating myelination. A recent study proposed that S1P treatment increases survival of mature oligodendrocytes via a pertussis-toxin-sensitive, Akt-dependent pathway.<sup>[9]</sup> S1P5 plays a role in these pro-survival effects of S1P, as S1P-mediated cell protection is attenuated after oligodendrocytes are treated with RNAi against S1P5.<sup>[9]</sup>

In oligodendrocyte preparations from newborn rat cortices, S1P5 protein was detected, and this was paralleled by expression of myelin basic protein (MBP, data not shown). In those cultures, FTY720-P as well as **1L** significantly increased the number of MBP-positive mature oligodendrocytes (Figure 3) at

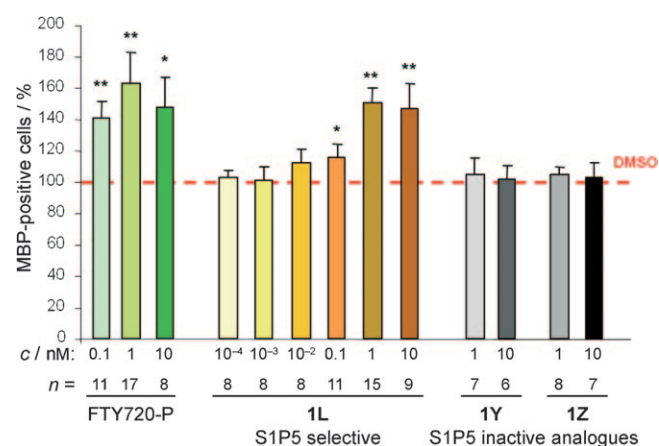


**Figure 3.** Effects of FTY720-P and **1L** (concentrations indicated) on the number of mature oligodendrocytes in vitro.<sup>[21]</sup> Error bars indicate  $\pm$  SEM; \* $p < 0.05$ , \*\* $p < 0.01$ .

very low concentrations, suggesting that both the S1P1 and S1P5 receptors contribute to the effect. This finding was recently confirmed by an independent research group, who demonstrated that **1L** rescued human adult mature oligodendrocytes from serum- and glucose-deprivation-induced cell death.<sup>[22]</sup>

The genetic ablation of S1P5 in vivo did not affect the myelination process.<sup>[9]</sup> Assuming S1P5 receptor stimulation promotes oligodendrocyte survival in vivo, as observed in vitro,

then FTY720-P and the novel S1P5 agonists described herein may directly promote myelination. Importantly, these S1P5 agonists may therefore be beneficial in the treatment of demyelinating disorders such as multiple sclerosis.

**Keywords:** agonists • FTY720 • myelination • oligodendrocytes • receptors • sphingosine

- [1] V. Brinkmann, M. D. Davis, C. E. Heise, R. Albert, S. Cottens, R. Hof, C. Bruns, E. Prieschl, T. Baumruker, P. Hiestand, C. A. Foster, M. Zollinger, K. R. Lynch, *J. Biol. Chem.* **2002**, *277*, 21453–21457.
- [2] B. Zemann, B. Kinzel, M. Muller, R. Reuschel, D. Mechtcheriakova, N. Urtz, F. Bornancin, T. Baumruker, A. Billich, *Blood* **2006**, *107*, 1454–1458.
- [3] M. H. Graler, E. J. Goetzl, *FASEB J.* **2004**, *18*, 551–553.
- [4] J. Chun, J. A. Weiner, N. Fukushima, J. J. Contos, G. Zhang, Y. Kimura, A. Dubin, I. Ishii, J. H. Hecht, C. Akita, D. Kaushal, *Ann. N. Y. Acad. Sci.* **2006**, *905*, 110–117.
- [5] N. Young, J. R. Van Brocklyn, *Exp. Cell Res.* **2007**, *313*, 1615–1627.
- [6] J.-L. Liao, Y.-T. Huang, H. Lee, *Zoological Studies* **2005**, *44*, 219–227.
- [7] F. Mullershausen, L. M. Craveiro, Y. Shin, M. Cortes-Cros, F. Bassilana, M. Osinde, W. Wishart, D. Guerini, M. Thallmair, M. E. Schwab, R. Sivasankaran, K. K. Dev, *J. Neurochem.* **2007**, *102*, 1151–1161.
- [8] H. S. Saini, R. P. Coelho, S. K. Goparaju, P. S. Jolly, M. Maceyka, S. Spiegel, C. Sato-Bigbee, *J. Neurochem.* **2005**, *95*, 1298–1310.
- [9] C. Jaillard, S. Harrison, B. Stankoff, M. S. Aigrot, A. R. Calver, G. Duddy, F. S. Walsh, M. N. Pangalos, N. Arimura, K. Kaibuchi, B. Zalc, C. Lubetzki, *J. Neurosci.* **2005**, *25*, 1459–1469.
- [10] K. Sato, H. Tomura, Y. Igarashi, M. Ui, F. Okajima, *Biochem. Biophys. Res. Commun.* **1997**, *240*, 329–334.
- [11] J. Harada, M. Foley, M. A. Moskowitz, C. Waerber, *J. Neurochem.* **2004**, *88*, 1026–1039.
- [12] T. D. Werry, G. F. Wilkinson, G. B. Willars, *Biochem. J.* **2003**, *374*, 281–296.
- [13] K. Palczewski, T. Kumasaka, T. Hori, C. A. Behnke, H. Motoshima, B. A. Fox, I. Le Trong, D. C. Teller, T. Okada, R. E. Stenkamp, M. Yamamoto, M. Miyano, Masashi, *Science* **2000**, *289*, 739–745.
- [14] D. S. Im, J. Clemens, T. L. Macdonald, K. R. Lynch, *Biochemistry* **2001**, *40*, 14053–14060.
- [15] D. S. Im, A. R. Ungar, K. R. Lynch, *Biochem. Biophys. Res. Commun.* **2000**, *279*, 139–143.
- [16] R. L. Malek, R. E. Toman, L. C. Edsall, S. Wong, J. , C. A. Letterle, J. R. Van Brocklyn, S. Milstien, S. Spiegel, N. H. Lee, *J. Biol. Chem.* **2001**, *276*, 5692–5699.
- [17] K. Terai, T. Soga, M. Takahashi, M. Kamohara, K. Ohno, S. Yatsugi, M. Okada, T. Yamaguchi, *Neuroscience* **2003**, *116*, 1053–1062.
- [18] A. Niedernberg, C. R. Scherer, A. E. Busch, E. Kostenis, *Biochem. Pharmacol.* **2002**, *64*, 8, 1243–1250.
- [19] M. Glickman, R. L. Malek, A. E. Kwitek-Black, H. J. Jacob, N. H. Lee, *Mol. Cell. Neurosci.* **1999**, *14*, 141–152.
- [20] N. Yu, K. D. Lariosa-Willingham, F. F. Lin, M. Webb, T. S. Rao, *Glia* **2004**, *45*, 17–27.
- [21] C. Barske, M. Osinde, C. Klein, H. Mattes, A. K. Mir, K. K. Dev, F. Gasparini, 60th Annual Meeting of the American Academy of Neurology, Chicago, IL (USA), **2008**, P089.
- [22] V. E. Miron, J. A. Hall, T. E. Kennedy, B. Soliven, J. P. Antel, *Am. J. Pathol.* **2008**, *173*, 1143–1152.

Received: June 15, 2010

Revised: July 26, 2010

Published online on September 2, 2010